High precision attitude estimation algorithm for SINS/CNS integrated navigation with unknown noise characteristics

Jiaqian Si*[a], Xuan Wang[b], Yanxiong Niu[a]
[a]School of Instrumentation Science and Opto-Electronic Engineering, Beihang University, Beijing 100191, China; [b]Shanghai Radio Equipment Research Institute, Shanghai 201109, China

ABSTRACT

Accurate attitude estimation is critical for the navigation systems of ballistic missiles. The SINS/CNS is commonly utilized in missiles. When noise parameters are unknown or changing over time, a single Kalman filter cannot meet the accuracy requirements. Hence, this paper explores an improved multi-model adaptive estimation (IMMAE) algorithm incorporating weight parameters to improve the accuracy. The optimized estimation is obtained through a weighted sum of sub-filters with different weight parameters. Additionally, the IMMAE algorithm effectively monitors noise and exhibits rapid adaptability of weight parameters under varying conditions. The simulation results demonstrate superior performance and enhanced adaptability of IMMAE algorithm compared to traditional Kalman filter and MMAE algorithms.

Keywords: SINS/CNS integrated navigation, Kalman filter, multi-model adaptive estimation, weight parameters

1. INTRODUCTION

As an autonomous navigation system, the strap-down inertial navigation system (SINS) is commonly utilized for high-precision attitude information in missiles without relying on external inputs [1-5]. Due to the integration principle employed in inertial navigation computation, errors in inertial devices will accumulate over time[6]. Celestial Navigation System (CNS) is suitable for prolonged autonomous operation of aerospace carriers for the advantages such as non-accumulation of navigation errors over time and high positioning accuracy. Therefore, SINS/CNS integrated navigation systems have extensive applications in missile systems[7,8].

The missile attitude accuracy is significantly influenced by the filtering algorithm. Kalman filter is commonly employed in SINS/CNS integrated navigation systems[9,10]. In current study, the conventional approach for designing the Kalman filter typically involves the utilization of fixed parameters[11]. The statistical characteristics and correlations of system noise are theoretically assumed to be accurately known[12]. However, due to the complexity of deep space exploration environment, as well as the lack of prior statistical knowledge, it is a formidable task to accurately determine the statistical characteristics of the navigation system noise. Various uncertain factors affect the performance of the navigation filtering algorithms, such as external interference or internal variations[13-15]. When the noise parameters fail to describe the dynamic model of the system precisely, the attitude errors increase and filtering outcomes diverge[16].

Nowadays, numerous research studies concentrating on adaptive filtering algorithm have been conducted to overcome the problem of the uncertainty noise[17]. Parameter adaptation and model adaptation are two pivotal aspects of ongoing research on adaptive Kalman filtering algorithms[12,18]. Ding proposed a Bayesian adaptive Kalman filter to estimate noise parameters. However, the algorithm imposed a requirement for high precision in the observed data[19]. Ge introduced an adaptive Cubature Kalman filter algorithm to estimate noise statistic property[12]. The computational complexity is increased in exchange for enhanced estimation performance by the algorithms. Besides, the researchers further proposed novel perspectives on these matters. Multiple model algorithm estimation (MMAE) is regarded as a promising research direction in the dynamic modeling and estimation of complex systems. It aims to adaptively estimate system parameters for unknown or uncertain systems by aggregating weighted estimates from filters with diverse parameter values. This facilitates better adaptation to system characteristics under various operating conditions[20,21].

As research continues, MMAE is applied in the aerospace domain, serving a critical function in achieving precise navigation and control. The allocation of weights is of utmost importance in MMAE, as it can significantly influence the performance and robustness of the filter[22]. Li conducted a series of research in view of the behavior of the model

*sijiaqianbuaa@163.com

International Conference on Optics, Electronics, and Communication Engineering (OECE 2024), edited by Yang Yue, Proc. of SPIE Vol. 13395, 1339507 · © 2024 SPIE · 0277-786X · Published under a Creative Commons Attribution CC-BY 3.0 License · doi: 10.1117/12.3049261

probability and stated that the model's weight is intricately linked to the performance of the multi-model algorithm[23]. Ormsby improved the MMAE framework by including probabilistic lower-bound techniques[24]. In the MMAE equation, the exponential component is essential for the calculation of probabilities. However, the presence of the determinant operator rapidly increases the weight which is closer to the actual model, resulting in unsatisfactory performance. Song proposed a novel multi-model adaptive estimation method in SINS/GPS system with time-varying noise[11]. The method improved the navigation accuracy in dynamic conditions. In practice, when noise varying, certain inferior models sometimes may be assigned greater weights, leading to undesirable competition between models. The trend is challenging to reverse, even though the converged model is no longer considered as the optimal model. Therefore, additional research efforts are warranted to advance the development of adaptive filtering algorithms for multiple models.

The aforementioned issues being taken into consideration, this paper proposed an improved MMAE (IMMAE) algorithm in SINS/CNS for case with insufficient prior knowledge of noise or when there are changes in the noise characteristics. In the system, the traditional MMAE algorithm is employed. In order to deal with undesirable competition between models, an adaptive-weight model is utilized to assess reliability. As a result, the model quickly updates when the noise parameters vary. The algorithm is simulated within a missile's SINS/CNS system, and the results demonstrate that IMMAE significantly improves attitude angle estimation accuracy with remarkable adaptability. The main contributions of this article, in comparison to previous works, are as follows:

- Developing an MMAE framework in the SINS/CNS to enhance the system's adaptability to changing noise conditions, surpassing the capabilities of single-filter models.
- Conducting theoretical analysis on the challenge of altering model due to adverse competition among models, to establish a theoretical foundation for the IMMAE algorithm.
- Proposing an adaptive weighting algorithm to achieve rapid model matching under time-varying noise conditions.

The subsequent sections of this paper are structured as follows. The Kalman filter and IMMAE are introduced in Section 2, and in Section 3, we introduce the navigation model of a ballistic missile using SINS/CNS. Section 4 details the simulation experiments, and Section 5 provides the conclusion of this paper.

2. IMPROVED MULTI-MODEL ADAPTIVE ESTIMATION

2.1 Kalman filter

The Kalman filter is commonly employed for accurate estimation of location, attitude, and angle. In the Kalman filter, the system state and measurement equations are equations (1) and (2), where $X_k \in R^n$ and $z_k \in R^m$ indicate the vector representing the state in n-dimensions and the vector representing measurements in m-dimensions, respectively, while k denotes the discrete time index. The matrix $\Phi_{k,k-1}$ denotes the state transition, while H_k stands for the measurement matrix. Γ_{k-1} represents the system noise driven matrix. Additionally, W_{k-1} and V_k correspond to process and measurement noise, following a Gaussian distribution with variance matrixes of Q_k and R_k, as shown in Equation (3). $\hat{X}_{k/k-1}$ and $P_{k/k-1}$ represent the one-step prediction of state and covariance matrix, respectively, while K_k denotes the filter gain. $\hat{X}_k$ and P_k are the estimated state and covariance matrix. Based on equation (3), given the state estimation initial value $\hat{X}_0 = X_0$ and the covariance matrix initial value P_0, the recursive calculation of state estimation $\hat{X}_k$ is obtained according to the measurement z_k.

$$X_k = \Phi_{k,k-1} X_{k-1} + \Gamma_{k-1} W_{k-1} \tag{1}$$

$$z_k = H_k X_k + V_k \tag{2}$$

$$\begin{cases} \hat{X}_{k/k-1} = \Phi_{k,k-1} \hat{X}_{k-1} \\ P_{k/k-1} = \Phi_{k,k-1} P_{k-1} {\Phi_{k,k-1}}^T + \Gamma_{k-1} Q_{k-1} {\Gamma_{k-1}}^T \\ K_k = P_{k/k-1} H_k^T \left(H_k P_{k/k-1} H_k^T + R_k \right)^{-1} \\ \hat{X}_k = \hat{X}_{k/k-1} + K_k \left(z_k - H_k \hat{X}_{k/k-1} \right) \\ P_k = \left(I - K_k H_k \right) P_{k/k-1} \end{cases} \tag{3}$$

2.2 Improved multi-model adaptive estimation

The Kalman filter relies on fixed parameters and exhibits certain limitations in practical application. When uncertain factors exist in the system operating environment, these fixed parameters cannot accurately describe the system's current state. Thus, the estimation results may fail to accurately capture the system's current state, leading to potentially inaccurate or even divergent estimation results. The uncertainty in system characteristics is typically due to noise variation, so the system's performance is significantly influenced by the noise parameters precision.

The MMAE algorithm employs a set of parallel Kalman filters with varying noise parameters to achieve optimal estimation. These sub-filters operate in parallel to estimate the current state of filter models and generate their respective filtering values. The conditional probability of each filter model is determined based on the residuals of M filter models while calculating the weight values for the filter models at the current moment. The estimation result is obtained using a weighted sum of sub-filter results based on their corresponding weight values. Figure 1 illustrates the MMAE's flow chart.

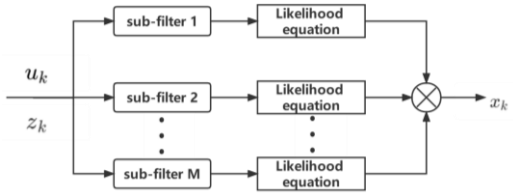

Figure 1. The flow chart for MMAE.

In the traditional MMAE algorithm[25], the weight of the filter model closest to the actual one converges to 1 at a rapid pace, while the weights of other filters tend to be 0. It causes MMAE to disregard information about the filters with low weight, imposing a slow response when noise changes. Hence, the developed IMMAE algorithm aims to overcome this problem by introducing an adaptive-weight model that assesses consistency between the current estimated model and the actual situation. If inconsistency is detected, the filter model weights are initialized accordingly. Additionally, different system noise variance matrices are assigned for varying interference amplitudes in equation (4), where Q_0 is the adjustable matrix. $\theta^{(\tau)}$ represents an element from the pre-set parameter set and τ denotes the model index. The corresponding sub-filter can be designed according to $\theta^{(\tau)}$.

$$Q_k^{(\tau)} = \theta^{(\tau)} Q_0 \quad \tau=1,2...M \tag{4}$$

The steps of IMMAE are as follows:

(1) Initialization

The state estimate initial value is set in equation (5) and the covariance initial value of estimation error in equation (6).

$$\hat{x}_0^{(\tau)} = \hat{x}_0 \tag{5}$$

$$P_0^{(\tau)} = P_0 \tag{6}$$

(2) Parallel filtering

At time k, each filter model individually predicts the state estimation and covariance. For the τ-*th* filter, the state estimate $\hat{x}_k^{(\tau)}$ and the corresponding error covariance $P_k^{(\tau)}$ are calculated using the following equations.

$$\hat{x}_{k|k-1}^{(\tau)} = \Phi_{k,k-1} \hat{x}_{k-1}^{(\tau)} \tag{7}$$

$$P_{k|k-1}^{(\tau)} = \Phi_{k,k-1} P_{k-1}^{(\tau)} (\Phi_{k,k-1})^T + Q_k^{(\tau)} \tag{8}$$

$$\hat{x}_k^{(\tau)} = \hat{x}_{k|k-1}^{(\tau)} + K_k^{(\tau)} [z_k - H_k \hat{x}_{k|k-1}^{(\tau)}] \tag{9}$$

$$K_k^{(\tau)} = P_{k|k-1}^{(\tau)} (H_k^{(\tau)})^T [H_k^{(\tau)} P_{k|k-1}^{(\tau)} (H_k^{(\tau)})^T + R_k]^{-1} \tag{10}$$

$$P_k^{(\tau)} = [I - K_k^{(\tau)} H_k^{(\tau)}] P_{k|k-1}^{(\tau)} [I - K_k^{(\tau)} H_k^{(\tau)}]^T + K_k^{(\tau)} R_k (K_k^{(\tau)})^T \tag{11}$$

(3) Weight update

The corresponding parallel Kalman filter computes the state estimation weights based on the residual measurement and covariance matrix. For the *τ-th* filter, the weight calculation formula is expressed as follows. Equation (12) represents the measurement residual matrix, while equation (13) describes the corresponding residual covariance matrix. The characteristics of a zero-mean Gaussian white noise sequence would be exhibited by the residual of this filter when the *τ-th* filter model aligns with the true system model. Therefore, the *τ-th* filter model's probability density function is mathematically expressed as equation (14).

$$\tilde{z}_k^{(\tau)} = z_k - H_k \hat{x}_{k|k-1}^{(\tau)} \tag{12}$$

$$\hat{\Omega}_k^{(\tau)} = H_k^{(\tau)} P_{k|k-1}^{(\tau)} (H_k^{(\tau)})^T + R_k \tag{13}$$

$$\Lambda_k^{(\tau)} = \frac{1}{\sqrt{|2\pi\hat{\Omega}_k^{(\tau)}|}} \exp[-\frac{1}{2}(\tilde{z}_k^{(\tau)})^T (\hat{\Omega}_k^{(\tau)})^{-1} \tilde{z}_k^{(\tau)}] \tag{14}$$

According to Bayes theorem, the recursive formula can calculate the posterior conditional probability. The values of $\omega_k^{(\tau)}$ and $\varpi_k^{(\tau)}$ can be obtained through equations (15) and (16). In the IMMAE algorithm, the model's initial weight $\omega_0^{(\tau)}$ is assigned as 1/*M*, while the initial weight $\varpi_0^{(\tau)}$ of the adaptive-weight model is also assigned as 1/*M*.

$$\omega_k^{(\tau)} = \frac{\omega_{k-1}^{(\tau)} \Lambda_k^{(\tau)}}{\sum_{\tau=1}^{M} \omega_{k-1}^{(\tau)} \Lambda_k^{(\tau)}} \tag{15}$$

$$\varpi_k^{(\tau)} = \frac{\Lambda_k^{(\tau)}}{\sum_{\tau=1}^{M} \varpi_{k-1}^{(\tau)} \Lambda_k^{(\tau)}} \varpi_{k-1}^{(\tau)} \tag{16}$$

(4) Output

The IMMAE algorithm's output is the sum of state estimations obtained from multiple parallel filters with corresponding weights, which is expressed as equation (17). The corresponding error covariance matrix is expressed as equation (18).

$$\hat{x}_k = \sum_{\tau=1}^{M} \omega_k^{(\tau)} \hat{x}_k^{(\tau)} \tag{17}$$

$$P_k = \sum_{\tau=1}^{M} \omega_k^{(\tau)} [P_k^{(\tau)} + (\hat{x}_k - \hat{x}_k^{(\tau)})(\hat{x}_k - \hat{x}_k^{(\tau)})^T] \tag{18}$$

(5) Assessment of IMMAE model reliability

The reliability of the current model is evaluated after a defined interval of time, denote as *T*, based on the relationship between $\omega_k^{(\tau)}$ and $\varpi_k^{(\tau)}$. If the maximum value of the filter model weight ω_k exceeds the threshold value and the corresponding filter model differs from adaptive-weight model, then reset $\omega_k^{(\tau)}$ to 1/*M*. At the same time, reset $\varpi_k^{(\tau)}$ to 1/*M*.

3. SINS/CNS INTEGRATED NAVIGATION MODEL

3.1 Equation of state

In the ballistic missile system, the equation of state is established within the reference frame of launch inertial coordinates[26], as shown in equation (19). $X(t)$ is the system state vector and it is expressed in equation (20), where [ϕ_x ϕ_y ϕ_z] denotes the misalignment angles, [δV_x δV_y δV_z] is the velocity error vector. [δx δy δz] denotes the vector indicating

position error, [ε_x ε_y ε_z] denotes constant drift of the gyroscope, and the accelerometer constant bias is expressed as [∇_x ∇_y ∇_z]. The system matrix $F(t)$ and system noise driven matrix $G(t)$ are expressed as equations (21) and (22), where the matrix C_b^{li} denotes the transformation between the body coordinate system and the launch inertial frame (i-frame), F_a and F_b are expressed as equations (23) and (24).

$$\dot{X}(t) = F(t)X(t) + G(t)W(t) \tag{19}$$

$$X(t) = [\phi_x \ \phi_y \ \phi_z \ \delta V_x \ \delta V_y \ \delta V_z \ \delta x \ \delta y \ \delta z \ \varepsilon_x \ \varepsilon_y \ \varepsilon_z \ \nabla_x \ \nabla_y \ \nabla_z]^T \tag{20}$$

$$F(t) = \begin{bmatrix} 0_{3\times3} & 0_{3\times3} & 0_{3\times3} & C_b^{li} & 0_{3\times3} \\ F_b & 0_{3\times3} & F_a & 0_{3\times3} & C_b^{li} \\ 0_{3\times3} & I_{3\times3} & 0_{3\times3} & 0_{3\times3} & 0_{3\times3} \\ 0_{3\times3} & 0_{3\times3} & 0_{3\times3} & 0_{3\times3} & 0_{3\times3} \\ 0_{3\times3} & 0_{3\times3} & 0_{3\times3} & 0_{3\times3} & 0_{3\times3} \end{bmatrix} \tag{21}$$

$$G(t) = \begin{bmatrix} C_b^{li} & 0_{3\times3} \\ 0_{3\times3} & C_b^{li} \\ 0_{3\times3} & 0_{3\times3} \\ 0_{3\times3} & 0_{3\times3} \\ 0_{3\times3} & 0_{3\times3} \end{bmatrix} \tag{22}$$

$$F_a = \begin{bmatrix} f_{14} & f_{15} & f_{16} \\ f_{24} & f_{25} & f_{26} \\ f_{34} & f_{35} & f_{36} \end{bmatrix} \tag{23}$$

$$F_b = \begin{bmatrix} 0 & a_z & -a_y \\ -a_z & 0 & a_x \\ a_y & -a_x & 0 \end{bmatrix} \tag{24}$$

where

$$\begin{cases} f_{14} = -\dfrac{GM}{l^3}(1-3\dfrac{x^2}{l^2}) & f_{15} = 3\dfrac{GM}{l^3}\dfrac{x(y+R_0)}{l^2} & f_{16} = 3\dfrac{GM}{l^3}\dfrac{xz}{l^2} \\ f_{24} = f_{15} & f_{25} = -\dfrac{GM}{l^3}(1-3\dfrac{(y+R_0)^2}{l^2}) & f_{26} = 3\dfrac{GM}{l^3}(\dfrac{(y+R_0)z}{l^2}) \\ f_{34} = f_{16} & f_{35} = f_{26} & f_{36} = -\dfrac{GM}{l^3}(1-3\dfrac{x^2}{l^2}) \end{cases}.$$

$$l=(x^2+(y+R_0)^2+z^2)^{0.5}$$

$$a = \begin{bmatrix} a_x \\ a_y \\ a_z \end{bmatrix}$$

a is the apparent acceleration. The gravitational constant in a geocentric model is represented as GM, while R_0 stands for the radius of curvature of the meridian at the launch location, and x, y, z indicate the missile's position within the i-frame coordinate system.

The system noise is $W(t) = \left[\omega_{\varepsilon_x} \ \omega_{\varepsilon_y} \ \omega_{\varepsilon_z} \ \omega_{\nabla_x} \ \omega_{\nabla_y} \ \omega_{\nabla_z}\right]^T$, where $[\omega_{\varepsilon_x}, \omega_{\varepsilon_y}, \omega_{\varepsilon_z}]$ represents the gyroscope random errors and $[\omega_{\nabla_x}, \omega_{\nabla_y}, \omega_{\nabla_z}]$ is the accelerometer random drifts matrix.

3.2 Measurement equation

The star sensor's output reflects the attitude of the carrier. The misalignment angles ϕ_x, ϕ_y, and ϕ_z in the mathematics platform is considered as observed quantities in measurement equation. Therefore, the measurement equation $Z(t)=[\phi_x\ \phi_y\ \phi_z]^T=HX(t)+V(t)$. In the equation, $H=[I_{3\times3}\ 0_{3\times3}\ 0_{3\times9}]$, $V=[\Delta X_S\ \Delta Y_S\ \Delta Z_S]^T$. V denotes the measurement noise of star sensor.

4. SIMULATION EXPERIMENT

This section presents the designed simulation system for the ballistic missile's integrated SINS/CNS navigation system. Then, we apply the Kalman filter, MMAE, and IMMAE for information fusion, and finally, we compare and analyse the performance of the competitor methods.

4.1 Simulation conditions

The simulation lasts for 600 s, and the trajectory is planned based on the actual flight of the missile., with its parameters reported in Table 1. Figure 2 illustrates the flow chart of the SINS/CNS integrated navigation simulation. To align with the IMMAE algorithm fidelity to real conditions, five models are developed, which have the following covariance matrices for process noise: Q_0, $10Q_0$, 10^2Q_0, 10^3Q_0, and 10^4Q_0.

The initial estimation of the state, along with its covariance and the variance of system noise, are configured as $P_{0|0}=diag([(6/180/3600*\pi)^2,\ (10/180/3600*\pi)^2,\ (10/180/3600*\pi)^2,\ 0.1^2,\ 0.1^2,\ 0.1^2,\ 5^2,\ 5^2,\ 5^2,\ (0.5/180/3600*\pi)^2,\ (0.5/180/3600*\pi)^2,\ (0.5/180/3600*\pi)^2,\ (5\times10^{-4}g_0)^2,\ (5\times10^{-4}g_0)^2,\ (5\times10^{-4}g_0)^2])$ and $Q_0=diag([(\pi/180/3600)^2,\ (\pi/180/3600)^2,\ (\pi/180/3600)^2,\ (5\times10^{-4}g_0)^2,\ (5\times10^{-4}g_0)^2,\ (5\times10^{-4}g_0)^2])$, where $g_0=9.7803267714$.

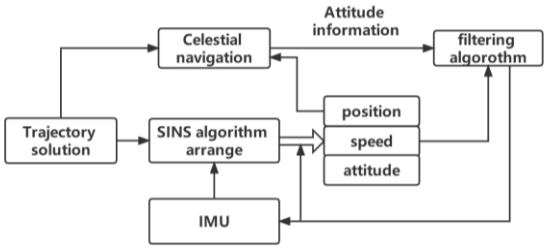

Figure 2. Simulation flow chart of SINS/CNS integrated navigation.

Table 1. The initial parameters.

Parameter	Value
Output frequency of INS	100 Hz
Filter period	0.05 s
Initial pitch angle	90°
Latitude of the launch point	39.98°
Longitude of the launch point	116.34°
Total flight time	600 s
Random noises from the gyroscope	1°/h
Random noises from the accelerometer	$5\times10^{-4}g_0$
Gyro constant drift	0.5°/h
Accelerometer constant bias	$1\times10^{-4}g_0$
Random noises of star sensor	1″
Initial angle of deviation	(10″,6″,10″)

4.2 Results and analysis

In order to illustrate the advantages and disadvantages of various methods, we evaluate the navigation property of these filtering algorithms in terms of Root Mean Square Error (RMSE), which is expressed as equation (25). n denotes the quantity of accessible experimental data, while Δ_i signifies the discrepancy between the true and estimation values.

$$RMSE = \sqrt{\frac{1}{n}\sum_{i=1}^{n}\Delta_i} \tag{25}$$

(1) Simulation 1

The actual system noise variance matrix is Q_0, while the noise covariance matrix of the single filter is $4Q_0$ due to inaccurate noise estimation. Figure 3 illustrates the errors of different estimation methods, with relevant details magnified for clarity. Table 2 reports the corresponding RMSEs. Based on the simulation results, the proposed IMMAE algorithm outperforms a single Kalman filter by exhibiting fewer errors and higher precision. Specifically, the attitude angles for the Kalman filter have an RMSE of 0.18296, 0.17572, and 0.17851, respectively, while the proposed method attains 0.16666, 0.15636, and 0.16422. The precision of attitude angles increases by 8.91%, 11.02%, and 8.01%. When faced with unknown or inaccurate system noise, the IMMAE demonstrates superior performance compared to a single Kalman filter. Figure 4 depicts the weights of the five models in the IMMAE method. During the filtering process of IMMAE, the weight of model 1 with the process noise matrix Q_0 approaches 1 rapidly, while the weight of other models decreases to approximately 0. Hence, it is evident that IMMAE accurately estimates the system noise and filters it accurately.

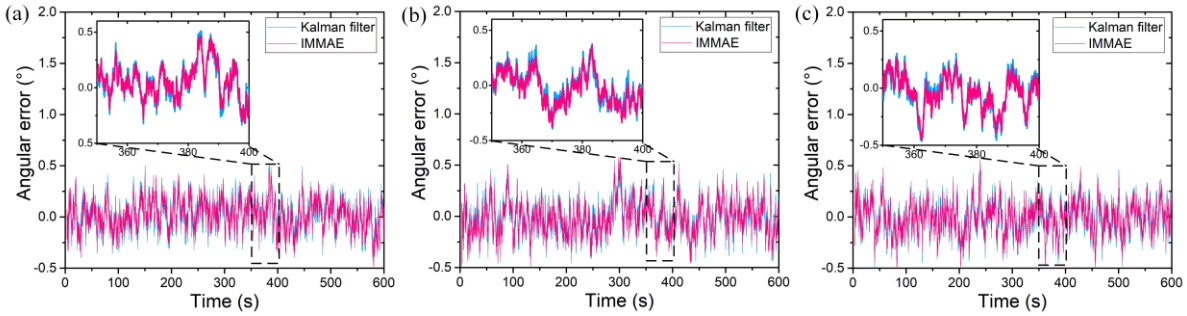

Figure 3. Angular errors in simulation 1. (a): yaw; (b): pitch; (c): roll.

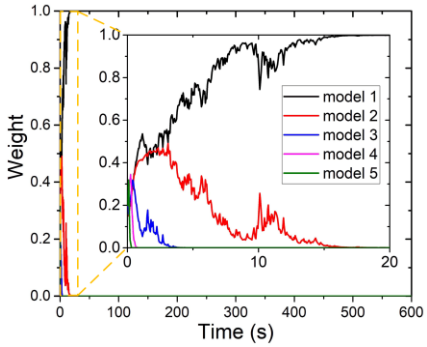

Figure 4. Weight value of the model of IMMAE in simulation 1.

Table 2. Performance of different filtering methods in simulation 1.

Filter	RMSE of the yaw angle (″)	RMSE of the pitch angle (″)	RMSE of the roll angle (″)
Kalman filter	0.18296	0.17572	0.17851
IMMAE	0.16666	0.15636	0.16422

(2) Simulation 2

The real system noise variance matrix is Q_0 in the first 200 s and the last 200 s, and $10Q_0$ in the 200-400 s. Figure 5 reveals the errors of different filters, while Table 3 presents the corresponding RMSEs of the orientation angles in varying scenarios. The results demonstrate that the proposed IMMAE algorithm outperforms the single Kalman filter and MMAE. During the time intervals of 0-200 s and 400-600 s, the filtering accuracy achieved by both the single Kalman filter and IMMAE is comparable due to the accurate noise estimation. However, between the 200 s and 400 s, the error of the single Kalman filter increases because it relies on the fixed parameters. In contrast, IMMAE exhibits rapid model-switching capability, maintaining an accurate filtering effect. The yaw, pitch, and roll angles derived from the Kalman filter yielded RMSEs of 0.21911, 0.26309, and 0.25783 respectively after 600 simulation iterations. Similarly, the MMAE approach provided RMSEs of 0.21413, 0.22653, and 0.22957 for yaw, pitch, and roll angles, respectively. In contrast to the competitor methods, the proposed IMMAE algorithm achieved significantly lower RMSEs of 0.19681 (10.18% improvement), 0.20683 (21.38% improvement), and 0.21063 (18.31% improvement) for yaw, pitch, and roll angles, respectively.

Table 3. Performance of different filtering methods in simulation 2.

Filter	RMSE of the yaw angle (″)	RMSE of the pitch angle (″)	RMSE of the roll angle (″)
Kalman filter	0.21911	0.26309	0.25783
MMAE	0.21413	0.22653	0.22957
IMMAE	0.19681	0.20683	0.21063

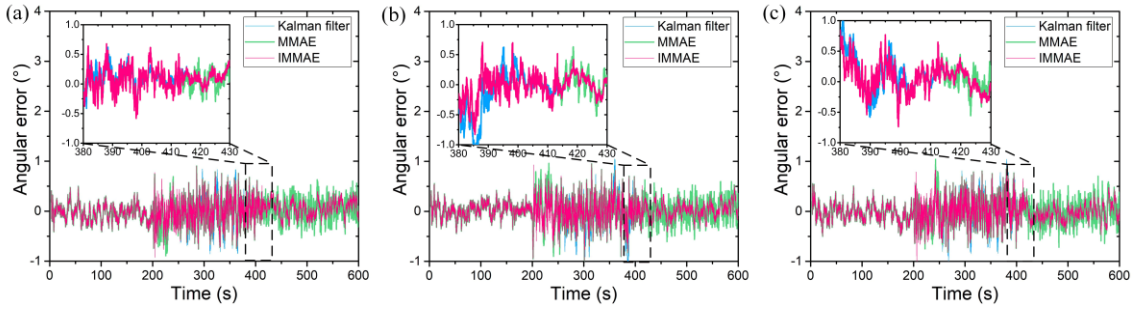

Figure 5. Angular errors in simulation 2. (a): yaw; (b): pitch; (c): roll.

Figure 6a illustrates the weight variations of each traditional MMAE model, highlighting that MMAE algorithm exhibits limited responsiveness to changes in system noise. Figure 6b depicts the weight profiles of each IMMAE model. Notably, during the time interval of 200-400 s, the weight of model 2 approaches 1 rapidly while the weight of other models converges to 0. Consequently, even when confronted with fluctuations in system noise, IMMAE algorithm consistently demonstrates superior filtering performance compared to single Kalman filter and MMAE algorithm approaches.

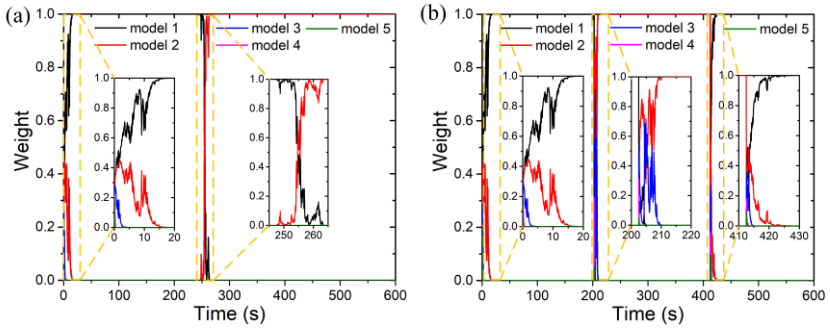

Figure 6. Weight value of the models in simulation 2 in (a) MMAE (b) IMMAE.

5. CONCLUSION

This study proposes a SINS/CNS integrated navigation algorithm utilizing an IMMAE method, effectively mitigating the impact of uncertainty and variations in noise characteristics. When the system noise is inaccurate, the proposed method reduces the estimation error by accurately tracking the system noise. Moreover, the IMMAE algorithm effectively addresses the limitation of traditional MMAE methods in model-switching when confronted with changes in system noise. The simulations in various conditions demonstrate the exceptional precision and adaptability of IMMAE algorithm.

REFERENCES

[1] Wang, D., Lv, H. and Wu, J., "A novel SINS/CNS integrated navigation method using model constraints for ballistic vehicle applications," J. Navigation 70, 1415-1437 (2017).

[2] Tang, C., Chen, L. and Chen, J., "Efficient coning algorithm design from a bilateral structure," Aerospace Science and Technology 79 48-57 (2018).

[3] Zhang, Y., Shen, C., Tang, J. and Liu. J., "Hybrid algorithm based on MDF-CKF and RF for GPS/INS system during GPS outages (April 2018)," IEEE Access 6, 35343-35354 (2018).

[4] Zhu, Z., Li, C. and Ye, W., "A dual-rate hybrid filtering method to eliminate high-order position errors of GPS in POS," Aerospace Science and Technology 78, 43-53 (2018).

[5] Li, J., Wang, Y., Lu, Z. and Li, Y., "Instantaneous observable degree modeling based on movement measurement for airborne POS," Aerospace Science and Technology 84, 916-925 (2019).

[6] Ma, Y., Fang, J., Wang, W. and Li, J., "Decoupled observability analyses of error states in INS/GPS integration," J. Navigation 67, 473-494 (2014).

[7] Ning, X., Gui, M., Xu, Y., Bai, X. and Fang, J., "INS/VNS/CNS integrated navigation method for planetary rovers," Aerospace Science and Technology 48, 102-114 (2016).

[8] Ning, X. and Liu, L., "A Two-Mode INS/CNS navigation method for lunar rovers," IEEE Trans. Instrum. Meas. 63, 2170-2179 (2014)

[9] Qian, H., Sun, L., Cai, J. and Peng. Y., "A novel navigation method used in a ballistic missile," Meas. Sci. Technol. 24, 105011 (2013).

[10] Xiong, K., Wei, C. L. and Liu, L. D., "Robust multiple model adaptive estimation for spacecraft autonomous navigation," Aerospace Science and Technology 42, 249-258 (2015).

[11] Song, J., Li, J., Wei, X., Hu, C., Zhang, Z., Zhao, L. and Jiao, Y., "Improved multiple-model adaptive estimation method for integrated navigation with time-varying noise," Sensors 22, 5976 (2022).

[12] Ge, Q., Ma, Z., Li, J., Yang, Q., Lu, Z. and Li, H., "Adaptive cubature Kalman filter with the estimation of correlation between multiplicative noise and additive measurement noise," Chinese Journal of Aeronautics 35, 40-52 (2022).

[13] Youn, W., Ko, N. Y., Gadsden, S. A. and Myung, H., "A novel multiple-model adaptive Kalman filter for an unknown measurement loss probability," IEEE Trans. Instrum. Meas. 70, 1-11 (2021).

[14] Chen, J., Hou, X., Qin, Z. and Guo, R., "A novel adaptive estimator for maneuvering target tracking," In 2007 International Conference on Mechatronics and Automation 3756-3760 (2007).

[15] Yunita, M., Suryana, J. and Izzuddin, A., "Error performance analysis of IMM-Kalman filter for maneuvering target tracking application," In 2020 6th International Conference on Wireless and Telematics (ICWT), 1-6 (2020).

[16] Fan, X., Wang, G., Han, J. and Wang, Y., "Interacting multiple models based on maximum correntropy Kalman filter," IEEE Trans. Circuits Syst. II 68, 3017-3021 (2021).

[17] Alsuwaidan, B. N., Crassidis, J. L. and Cheng, Y., "Generalized multiple-model adaptive estimation using an autocorrelation approach," IEEE Trans. Aerosp. Electron. Syst. 47, 2138-2152 (2011).

[18] Chernikova, O. S. and Grechkoseev, A. K., "Two-stage parametric identification procedure for a satellite motion model based on adaptive unscented Kalman filters," Bulletin of the SUSU. MMP 15, 4 (2022).

[19] Ding, D., He, K. F. and Qian, W. Q., "A bayesian adaptive unscented Kalman Filter for aircraft parameter and noise estimation," Journal of Sensors 2021, 1-11 (2021).

[20] Magill, D., "Optimal adaptive estimation of sampled stochastic processes," IEEE Trans. Automat. Contr. 10, 434-439 (1965).

[21] Kottath, R., Poddar, S., Das, A. and Kumar, V., "Window based multiple model adaptive estimation for navigational framework," Aerospace Science and Technology 50, 88-95 (2016).
[22] Maybeck, P. S. and Stevens, R. D., "Reconfigurable flight control via multiple model adaptive control methods," IEEE Trans. Aerosp. Electron. Syst. 27, 470-480 (1991).
[23] Zhao, Z. and Li, X. R., "The behavior of model probability in multiple model algorithms," In 2005 7th International Conference on Information Fusion, 6 (2005).
[24] Ormsby, C. D., "Generalized residual multiple model adaptive estimation of parameters and states," Air Force Institute of Technology, (2003).
[25] Li, X. and Jilkov, V. P., "Survey of maneuvering target tracking. part v: multiple-model methods," IEEE Trans. Aerosp. Electron. Syst. 41, 1255-1321 (2005).
[26] Quan, W., Gong, X., Fang, J. and Li, J., [INS/GNSS Integrated Navigation Method], Springer, Berlin & Heidelberg, 185-235 (2015).